CIRCUITS SYSTEMS SIGNAL PROCESSING
VOL. 26, NO. 1, 2007, PP. 27–42
© Birkhäuser Boston (2007)
DOI: 10.1007/s00034-005-0220-x

DESIGN EQUATIONS FOR JOINTLY OPTIMIZED FREQUENCY-RESPONSE MASKING FILTERS[1]*

Jianghong Yu[1] *and Yong Lian*[1]

Abstract. The introduction of nonlinear optimization techniques to the design of a frequency-response masking (FRM) filter has changed the way in which an FRM filter is synthesized. It allows all subfilters in an FRM structure to be optimized jointly, resulting in further savings in the number of arithmetic operations. Under the joint optimization, a new set of design equations is necessary, not only for a more computationally efficient filter, but also for the simplification of the design process and the reduction of the design time. In this paper, we present a set of design equations that estimates the filter lengths and optimum interpolation factor in an FRM filter under joint optimization. It is shown, by means of examples, that the proposed design equations lead to a better estimation of the optimum interpolation factor compared with existing design equations.
Key words: Digital filter, FIR filter, frequency-response masking (FRM), joint optimization.

1. Introduction

The frequency-response masking (FRM) approach is one of the most computationally efficient techniques for the design of linear-phase arbitrary bandwidth sharp FIR digital filters [1], [3]–[10], [12]–[29], [31]–[38]. A basic FRM filter contains four subfilters, i.e., a pair of complementary bandedge shaping filters $H_a(z)$ and $H_c(z)$ and two masking filters $H_{Ma}(z)$ and $H_{Mc}(z)$, as shown in Figure 1. The implementation of $H_c(z)$ is very simple and requires only one additional subtractor. To understand the principle of an FRM filter, let us consider the synthesis of a sharp lowpass FIR filter $H(z)$ with a normalized transition

* Received February 21, 2005; revised June 23, 2006; This work is supported by National University of Singapore Academic Research Fund R-263-000-291-112 and A*STAR TSRP grant 052-118-0060 under Embedded and Hybrid Systems II.

[1] Department of Electrical and Computer Engineering, National University of Singapore, Block E4, Level 5, Room 48, 4 Engineering Drive 3 Singapore 117576. E-mail for Yu: jhyu@jdl.ac.cn; E-mail for Lian: eleliany@nus.edu.sg

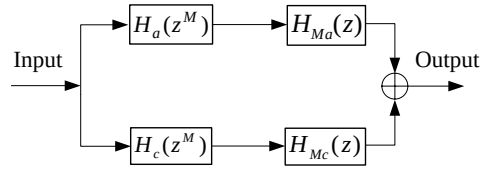

Figure 1. A basic realization structure for the FRM filter.

bandwidth of ΔF. The creation of an FRM filter starts with a bandedge shaping filter $H_a(z)$ and its complement $H_c(z)$ whose transition bandwidths are M times wider than that of the overall filter $H(z)$ as shown in Figure 2a. A pair of periodic narrow transition width filters $H_a(z^M)$ and $H_c(z^M)$ is created by interpolation, i.e., by replacing each delay element in both $H_a(z)$ and $H_c(z)$ with M delay elements, as shown in Figure 2b. The interpolation narrows the transition bandwidths of $H_a(z)$ and $H_c(z)$ by compressing their frequency responses, which produces extra passbands. Parts of these extra passbands fall into the stopband region of the overall filter. Two masking filters $H_{Ma}(z)$ and $H_{Mc}(z)$, as in Figure 2c, are cascaded to $H_a(z^M)$ and $H_c(z^M)$, respectively, to remove the unwanted passbands. The outputs of $H_{Ma}(z)$ and $H_{Mc}(z)$, are combined to form the overall filter, as shown in Figures 2d to f, respectively. The design equations and the derivation of optimum interpolation factors for single- and multiple-stage FRM filters can be found in [20], [21].

In an FRM filter, the savings in terms of number of multipliers are closely related to the interpolation factor applied to the bandedge shaping filter. A large interpolation factor reduces the complexity of the bandedge shaping filter at a cost of longer masking filters. There exists an optimum interpolation factor M_{opt} for a given set of specifications that leads to a minimum total number of coefficients in an FRM filter. Such an optimum M can be estimated using a formula given in [21]:

$$M_{opt} \approx \frac{1}{2\sqrt{\Delta F}}, \tag{1}$$

where ΔF is the normalized transition bandwidth of the FRM filter. The derivation of (1) is based on an assumption that the complexity of an FRM filter is minimized when the transition bandwidths of the two masking filters are the same. Such an assumption may not hold for the FRM filters designed using an iterative design procedure [21]. Nevertheless, (1) gives a good estimation of the optimum M and narrows the search region for optimum M to a few integers.

Much research effort has been made to improve the computational efficiency of FRM filters in recent years. A notable effort is to employ nonlinear optimization techniques to jointly optimize all subfilters in an FRM structure [26]–[28], [31], [33], [34], [38]. Such an approach leads to about 20% additional savings in terms of number of multipliers. However, it was reported in [31] that (1) is no longer accurate for an optimum M under the joint optimization. A new formula was

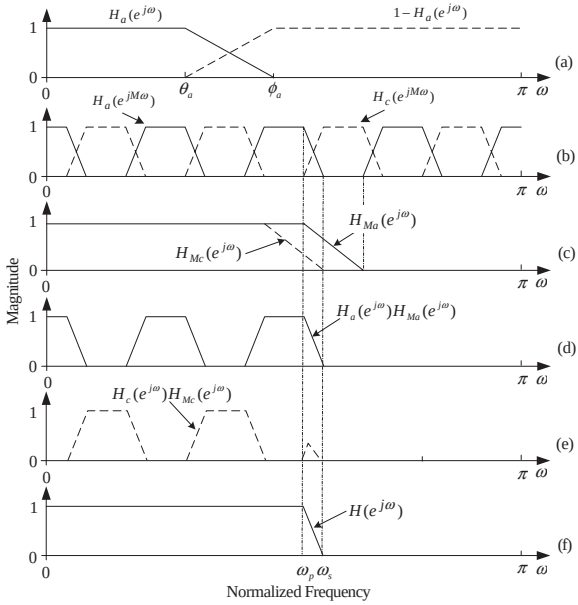

Figure 2. The frequency responses of various filters in the FRM approach.

given in [31]:

$$M_{opt} = \frac{1}{\sqrt{3.2\Delta F}}. \tag{2}$$

However, the authors of [31] did not show how accurate it is. In this paper, we present a new set of formulas for the estimation of filter lengths and the optimum M in a jointly optimized FRM filter. The new design equations are derived from the observations made for a few hundred FRM filters jointly optimized by a sequential quadratic programming (SQP) algorithm [2]. The proposed design equations lead to a better estimation of the interpolation factor than those reported in [20], [21], [31] and provide a guideline for determining the filter lengths of two masking filters, which speeds up the design process.

The rest of the paper is organized as follows. In Section 2, we highlight the differences between the original and jointly optimized FRM filters and discuss the impacts of joint optimization on the interpolation factor and subfilter lengths. In Section 3, we introduce a new filter length estimation equation for the bandedge shaping filter. In Section 4, further observations are made on the masking filters, and an equation is derived to estimate the total length of two masking filters. A new expression for the estimation of the optimum M is presented in Section 5. Design examples are presented in Section 6 which verify the accuracy of the proposed formulas. The conclusions are drawn in Section 7.

2. Impacts of joint optimization on FRM filters

A typical jointly optimized FRM filter employs three subfilters that have very different amplitude responses compared to those in the original FRM structure. This is due to the involvement of nonlinear optimization techniques that help in reshaping all subfilters in an FRM structure. As a result, the filter lengths of the subfilters are reduced. Figures 3a–e show the frequency responses of a typical FRM filter designed by the nonlinear optimization technique. It is obvious from Figures 3a and b that amplitude responses of the bandedge shaping filters are very different from those in the origianl FRM filter. Its normalized dc gain is no longer at 1, and the dc level is shifted. The ripple in the passband is considerably increased, especially towards the edges of the transition bands. Such changes have little impact on the filter length of the bandedge shaping filter according to design examples. But they affect the two masking filters greatly. The transition bandwidths of the masking filters are increased and become very close to each other as shown in Figure 3c. The widening of transition bandwidths in both masking filters has two effects on an FRM filter. It reduces the lengths of the two masking filters, which yields additional savings in the number of multipliers. At the same time, it leads to an increased interpolation factor such that the overall complexity of an FRM filter is reduced. The authors of [31] first noticed the increase in the interpolation factor and proposed the estimation formula (2). Design examples show that (2) gives a better estimation than that of (1). But the estimated value is still a short distance away from the optimum M and requires a few iterations to reach an optimum design.

The question is whether there is a need to develop a more accurate formula for the interpolation factor. To answer this question, let us examine how an FRM filter is designed using any of the joint optimization techniques. It starts with an initial solution that derives from one of the iterative design processes in [20], [21], [32], i.e., the interpolation factor is determined by a search method introduced in [21]. The initial filter lengths of bandedge shaping filter N_a and two masking filters N_{Ma} and N_{Mc} can be determined by assuming the ripple magnitude is 85% of the allowed ripple magnitude. Nonlinear optimization techniques are employed to jointly optimize all subfilters, leading to further reduction in the filter lengths after a few iterations. As the nonlinear optimization process does not include the interpolation factor M in the objective function, the resulting FRM filter is an improved version of the initial design. In order to find the best design, an exhaustive search is a must, which involves an iterative process, i.e., one must vary the M, calculate the filter lengths, jointly optimize all subfilters, and gradually reduce the length of each subfilter to reach a minimum complexity for a given M. This is a very time-consuming process. Thus, good estimations of the optimal interpolation factor and the filter lengths are necessary to simplify the design task.

To derive an interpolation factor estimation formula, we notice that the FRM filters designed with joint optimization methods coincide with the assumption

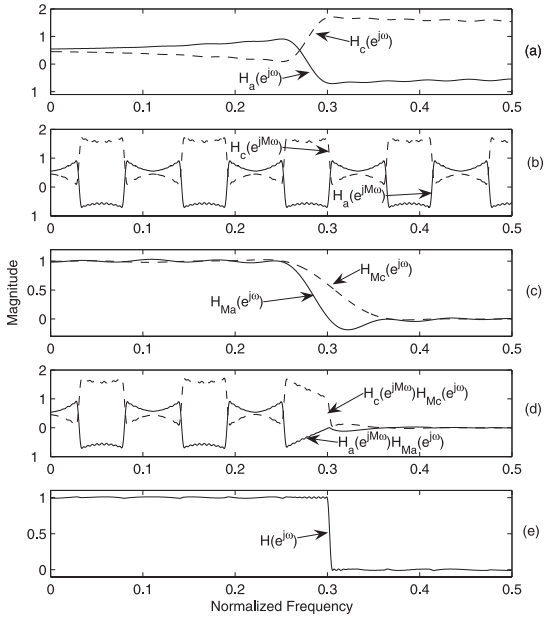

Figure 3. The frequency responses of various filters in jointly optimized FRM approach.

made in [21] about the masking filters, i.e., the transition bandwidths of two masking filters are the same for a minimum complexity FRM filter. It is clear from examples in [26], [27], [31], [33], [34], [38] that the transition bandwidths are almost the same for two masking filters. However, their lengths are not the same. This implies that the standard filter length estimation formula is no longer valid for subfilters in an FRM structure because the shapes of all the subfilters differ from that of the standard lowpass filters. Thus, new filter length estimation formulas are necessary to derive an optimum interpolation factor. Note from Figures 3a and c that the shape of the bandedge shaping filter differs from that of the two masking filters. We should develop the length estimations for the bandedge shaping filter and masking filters separately.

3. Filter length estimation for bandedge shaping filter

The filter length is normally determined by a set of filter specifications, i.e., the normalized passband and stopband edges f_p and f_s and the passband and stopband ripples δ_p and δ_s. The length estimation should be able to give a reasonably good match between the estimated length and actual filter length for a given set of specifications, i.e., varying the band edges or ripples should not affect the accuracy of the formula. For FRM filters, it is not necessary to develop the formula to cover all the normalized frequencies from 0 to 0.5. This is so

because the FRM approach is suitable for the synthesis of arbitrary bandwidth sharp transition bandwidth filters, mainly from moderate to wide bandwidths. For narrowband filters, the FRM approach simplifies to an interpolated finite impulse response structure [21], [30]. Therefore, we set the following restrictions for the FRM filters designed in the rest of this paper. The normalized passband edges are set in the region of $[0.1,\ 0.4]$. At the same time, the transition bandwidth of an FRM filter is limited to a range of $[0.002,\ 0.012]$. This region contains most designs for a single-stage FRM approach. To make sure that the developed formulas are accurate for different passband and stopband ripples, we vary the passband and stopband ripple from 10^{-1} to 10^{-5}. The passband edges and transition bandwidth are selected to be linearly distributed in the selected region, and passband and stopband ripples are logarithmically distributed. The interpolation factor M varies linearly between 4 to 20 based on the given transition bandwidth of $[0.002,\ 0.012]$. In this way, the gathered data become representative and reliable for the development of design equations for FRM filters.

Based on our experience, the length N_a of a jointly optimized bandedge shaping filter $H_a(z)$ is very close to one designed by traditional iterative methods. The main reason behind this phenomenon could be that the transition bandwidth of the bandedge shaping filter remains the same for both traditional and jointly optimized designs. In [20], N_a is estimated by assuming that the ripples of $H_a(z)$ are 85% of the allowed magnitude, and by using Kaiser's equation [11]. Therefore,

$$N_a(\Delta F, \delta_p, \delta_s) = \frac{-20\log_{10}\sqrt{\delta_p\delta_s} - 11.59}{14.6M\Delta F} + 1. \tag{3}$$

This equation is not very accurate if the length of the bandedge shaping filter is long. To improve its accuracy, we would like to modify the coefficients in Kaiser's equation, i.e.,

$$N_a(\Delta F, \delta_p, \delta_s) = \frac{k_1\log_{10}\sqrt{\delta_p\delta_s} - k_2}{k_3M\Delta F} + k_4, \tag{4}$$

where k_1, k_2, k_3, and k_4 are parameters to be determined. Note that δ_p and δ_s in the above equation are the passband and stopband ripples of the overall FRM filter, respectively. This applies to all equations in the following sections. A few hundred data points are collected from the FRM filters optimized with the SQP technique. The band edges, transition bandwidths, ripples, and interpolation factors are limited to the ranges described in the beginning of this section. k_1, k_2, k_3, and k_4 are obtained from collected data points using the method of least squares fitting. The modified formula is given by

$$N_a(\Delta F, \delta_p, \delta_s) = \frac{-9.9\log_{10}(\delta_p\delta_s) - 8.6}{16.3M\Delta F} + 3.33. \tag{5}$$

The distribution of the absolute errors, i.e., the difference between actual and estimated lengths based on (3) and (5), respectively, are calculated and listed in Table 1. From the table, it is clear that (5) provides a better estimation for the length of bandedge shaping filters than that of (3).

Table 1. Comparisons of design equations (3) and (5)

Absolute error	Equation (3)	Equation (5)
≤ 4	82.41%	88.96%
> 4	18.11%	11.04%

4. Masking filter length estimation

The estimation of length for each masking filter is a very difficult task based on our experience. We notice that the lengths of the two masking filters are exchangeable for many designs and the resultant overall filters satisfy the same specifications. To show this, let us consider the design of a lowpass filter with normalized passband and stopband edges at 0.191 and 0.197, respectively. The passband and stopband ripples are both 0.01. The optimum interpolation factor is 9 determined by exhaustive search. The lengths of three subfilters are $N_a = 39$, $N_{Ma} = 27$, and $N_{Mc} = 19$, where N_a is the length of the bandedge shaping filter, and N_{Ma} and N_{Mc} are the lengths of two masking filters. For the same M value, another set of subfilters can be found which satisfies the given specifications and uses the same number of coefficients as in the first design. The filter lengths are $N_a = 39$, $N_{Ma} = 19$, and $N_{Mc} = 27$. The lengths of the masking filters are swapped compared to the first design. Many other design examples we tried show the same property.

This phenomenon is very interesting and prompts us to find the sum of masking filter lengths instead of the individual length. Recall from [20] that the sum of transition bandwidths of masking filters is related to M, i.e.,

$$\Delta F_M = \Delta f_{Ma} + \Delta f_{Mc} = \frac{1}{M}, \tag{6}$$

where Δf_{Ma} and Δf_{Mc} are the transition bandwidths of two masking filters. We want to know if it is possible to use a modified Kaiser formula for the estimation of the sum of the masking filter lengths. Substituting (6) into Kaiser's formula, we have

$$N_{Msum} = N_{Ma} + N_{Mc} = kM \log_{10}(\delta_p \delta_s) - qM + c, \tag{7}$$

where N_{Ma} and N_{Mc} are the lengths of masking filters $H_{Ma}(z)$ and $H_{Mc}(z)$, respectively. k, q, and c are variables yet to be determined. To verify the validity of (7), let us carry out a few experiments. In each experiment, the FRM filters are optimized by SQP. One of the specifications among band edges, interpolation factor, and ripples is varied from one design to another while the remaining specifications are kept unchanged. The relationship between N_{Msum} and the selected specification is analyzed.

It is interesting to note that (7) is not a function of transition bandwidth. To gauge the impact of transition bandwidth on N_{Msum}, let us fix the passband edge,

Table 2. Filter specifications used in Figure 4

Legend	f_p	δ_p	δ_s	M	Legend	f_p	δ_p	δ_s	M
data1	0.11	0.05	0.005	11	data5	0.24	0.08	0.005	9
data2	0.14	0.01	0.001	12	data6	0.28	0.001	0.05	8
data3	0.16	0.03	0.001	10	data7	0.33	0.005	0.03	5
data4	0.21	0.01	0.01	6	data8	0.37	0.08	0.01	14

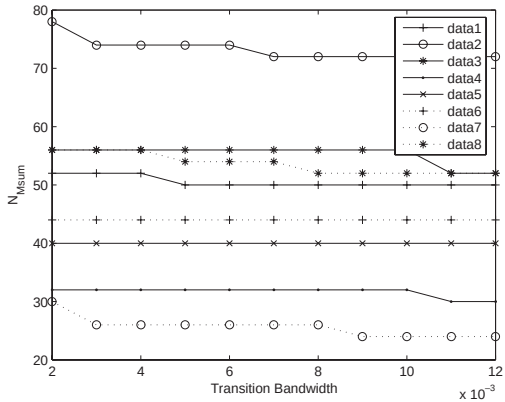

Figure 4. Relationship between N_{Msum} and transition bandwidth of the overall FRM filter.

ripples, and M as shown in Table 2 and vary the stopband edge. Figure 4 shows the relationship between N_{Msum} and the normalized transition bandwidth of FRM filters. It is clear that N_{Msum} is a constant if the change of transition bandwidth is limited to a small range. For a large range from 0.012 to 0.002, N_{Msum} varies a little in each data set. Therefore, it is safe to leave out the transition bandwidth in (7).

To verify the relationship between N_{Msum} and δ_s, we fix f_p, f_s, δ_p, and M as shown in Table 3. The δ_s is varied from 10^{-1} to 10^{-5}. The relationship between N_{Msum} and δ_s is plotted in Figure 5. It is obvious from Figure 5 that N_{Msum} changes linearly with the logarithm of stopband ripple δ_s or

$$N_{Msum} = k_1 \log_{10} \delta_s + c_1. \tag{8}$$

The same conclusion can be drawn for the passband ripple if we use the specifications listed in Table 4, i.e., varying δ_p from 10^{-1} to 10^{-5} while keeping the rest unchanged. Figure 6 confirms the linear relationship between N_{Msum} and the logarithm of passband ripple δ_p, i.e.,

$$N_{Msum} = k_2 \log_{10} \delta_p + c_2. \tag{9}$$

In (8) and (9) k_1, k_2, c_1, and c_2 are constants yet to be decided.

Table 3. Filter specifications used in Figure 5

Legend	f_p	f_s	δ_p	M	Legend	f_p	f_s	δ_p	M
data1	0.1	0.102	0.1	17	data5	0.26	0.265	0.02	9
data2	0.14	0.142	0.08	12	data6	0.3	0.306	0.01	11
data3	0.18	0.183	0.05	10	data7	0.34	0.347	0.008	8
data4	0.22	0.224	0.03	8	data8	0.38	0.388	0.005	7

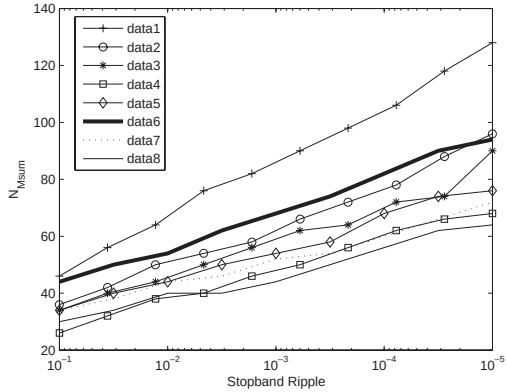

Figure 5. Relationship between N_{Msum} and stopband ripple.

Table 4. Filter specifications used in Figure 6

Legend	f_p	f_s	δ_s	M	Legend	f_p	f_s	δ_s	M
data1	0.12	0.122	0.1	15	data5	0.32	0.326	0.01	10
data2	0.17	0.173	0.05	10	data6	0.35	0.357	0.005	5
data3	0.21	0.214	0.03	11	data7	0.39	0.4	0.001	8
data4	0.26	0.265	0.02	9					

To show the relationship between N_{Msum} and M, we choose a set of lowpass filters with different band edges and passband and stopband ripples, as shown in Table 5. For each set of specifications, we design the FRM filters using SQP by varying M from 4 to 20. The sums of masking filter lengths are calculated and shown in Figure 7. It is not difficult to conclude from Figure 7 that the sum of masking filter lengths can be approximated by a linear relationship of M, i.e.,

$$N_{Msum} = k_3 M + c_3, \tag{10}$$

where k_3 and c_3 are constants yet to be found.

Equations (8), (9), and (10) confirm that (7) is valid. The values of k, q, and c in (7) can be determined by the method of least squares fitting. All the FRM filters

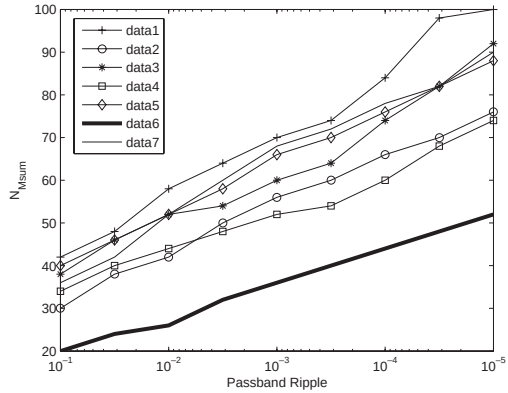

Figure 6. Relationship between N_{Msum} and passband ripple.

Table 5. Filter specifications used in Figure 7

Legend	f_p	f_s	δ_p	δ_s	Legend	f_p	f_s	δ_p	δ_s
data1	0.1	0.104	0.05	0.01	data4	0.25	0.257	0.001	0.05
data2	0.14	0.146	3.16×10^{-3}	0.001	data5	0.285	0.288	0.001	0.001
data3	0.18	0.185	0.01	0.01	data6	0.33	0.338	0.005	0.08

listed above and another few hundred FRM filters with different specifications have been designed by SQP. The selection of these specifications is described at the beginning of Section 3 and not repeated again. The obtained interpolation factor and filter lengths for the bandedge shaping filter and masking filters are used as data points for curve fitting. The final N_{Msum} is found to be

$$N_{Msum} = -1.15M\log_{10}(\delta_p\delta_s) + 0.02M + 5.24. \tag{11}$$

The second term in this equation is much smaller than the other two terms. By ignoring it, we obtain the final filter length sum estimation formula:

$$N_{Msum} = -1.15M\log_{10}(\delta_p\delta_s) + 5.24. \tag{12}$$

To verify the accuracy of (12), we have designed about 200 FRM filters with randomly selected filter specifications that comply with the constraints set in Section 3. The relative errors between the calculated values from (12) and the actual values of N_{Msum} of the selected designs have been calculated and the error distributions are listed in Table 6. It is clear that most of the estimations using (12) lead to less than 4% relative errors. We can comfortably say that design equation (12) is reliable.

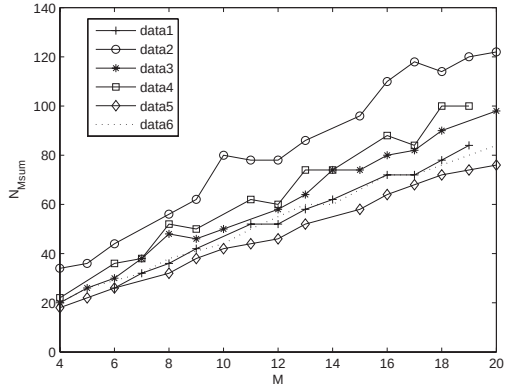

Figure 7. Relationship between the sum of masking filter lengths and interpolation factor M.

Table 6. Relative error distribution of equation (12)

Relative error	Percentage of total design examples
$\leq 4\%$	82.76%
$> 4\%$	17.24%

5. Optimum interpolation factor

Based on equations (5) and (12), the complexity of an FRM filter can be estimated by

$$\begin{aligned} N &= N_a + N_{Msum} \\ &= \frac{-9.9\log_{10}(\delta_p\delta_s)-8.6}{16.3M\Delta F} \\ &\quad -1.15M\log_{10}(\delta_p\delta_s) + 8.57. \end{aligned} \tag{13}$$

An optimum M that minimizes the N can be easily found from this equation if the partial derivative of N with respect to M is set to zero. This leads to the following equation:

$$M_{opt} = \sqrt{\frac{9.9\log_{10}(\delta_p\delta_s) + 8.6}{18.75\Delta F\log_{10}(\delta_p\delta_s)}}. \tag{14}$$

Generally speaking, $9.9\log_{10}(\delta_p\delta_s)$ is much larger than 8.6. If we ignore 8.6 and make a minor compensation, a simplified estimation of M_{opt} is obtained,

$$M_{opt} \approx \frac{1}{\sqrt{2.25\Delta F}}. \tag{15}$$

Table 7. Filter specifications for eight design examples

Design example	f_p	f_s	δ_p	δ_s
I	0.105	0.107	0.01	3.16×10^{-3}
II	0.145	0.149	0.01	3.16×10^{-3}
III	0.185	0.191	3.16×10^{-3}	3.16×10^{-3}
IV [31]	0.2	0.201	0.01	0.001
V	0.225	0.233	0.01	0.001
VI	0.265	0.274	0.0316	1.0×10^{-4}
VII [20]	0.3	0.305	0.01	0.01
VIII	0.385	0.388	0.01	0.01

6. Design examples

To verify the accuracy of the proposed design equations, we selected eight design examples with normalized passband edges ranging from 0.105 to 0.385 and normalized transition bandwidth from 0.001 to 0.009. Two of the examples were taken from [20] and [31], respectively. The details of the filter specifications are listed in Table 7. All filters were jointly optimized using the SQP technique. Table 8 shows the comparisons between the estimated filter design parameters and actual designs. It is clear from Table 8 that (15) gives a much better estimation of the interpolation factor than (1) [21] and (2) [31]. The estimated lengths of the bandedge shaping filters, N_a, are very close to those of the real designs. In fact, the differences between the estimated and actual lengths are less than 3 for all examples. The estimations for the total length of the two masking filters, N_{Msum}, show a significant improvement over that of Kaiser's equation (3). The new estimations are very close to the actual design, except for examples V and VI, where the relative errors are about 11% and 16%, respectively. Note that in example VI the optimal interpolation factor differs from the calculated one. This might be the reason why there is a large error in the estimation of the masking filter lengths.

The eight examples presented above show that the proposed design equations are accurate for the optimal interpolation factor and the length of the bandedge shaping filter. The estimated total masking filter length serves as a good starting point for the design of an FRM filter. Apart from the accuracy of the proposed design equations, the proposed (15) leads to designs with fewer coefficients. Taking example IV [31], the interpolation factor M estimated by (15) yields a design with a total of 257 coefficients, i.e., $N_a = 123$, $N_{Ma} = 56$, and $N_{Mc} = 78$. This compares favorably to the designs using interpolation factors of 16 and 18, which require totals of 266 coefficients ($N_a = 161$, $N_{Ma} = 48$, and $N_{Mc} = 58$)

Table 8. Comparisons of interpolation factor and filter lengths

Estimation and actual value	Design example							
	I	II	III	IV [31]	V	VI	VII [20]	VIII
Estimated M by (1) [21]	11	8	6	16	6	5	7	9
Estimated M by (2) [31]	12	9	7	18	6	6	8	10
Estimated M by proposed (15)	15	11	9	21	7	7	9	12
Actual optimum M	15	12	9	21	7	6	9	12
Estimated N_a by Kaiser's equation	77	49	50	126	48	56	44	55
Estimated N_a by proposed (5)	77	49	50	123	48	55	46	56
Actual length N_a	79	49	51	123	51	55	45	57
Estimated N_{Msum} by Kaiser's equation	235	112	102	228	114	101	73	119
Estimated N_{Msum} by proposed (12)	83	67	57	126	45	43	47	60
Actual length N_{Msum}	82	72	58	132	40	36	46	60

and 259 coefficients ($N_a = 149$, $N_{Ma} = 71$, and $N_{Mc} = 39$), respectively. Note that interpolation factor 16 is estimated by (1) [21] and 18 is found through (2) [31]. For design example VII [20], the best design requires 91 coefficients, i.e., $N_a = 45$, $N_{Ma} = 19$, $N_{Mc} = 27$, with an interpolation factor of 9 calculated using (15). For the interpolation factors of 7 and 8 estimated by (1) and (2), respectively, the corresponding designs use 95 coefficients ($N_a = 59$, $N_{Ma} = 11$, $N_{Mc} = 25$) and 93 coefficients ($N_a = 51$, $N_{Ma} = 27$, $N_{Mc} = 15$).

It is worth noting that the proposed design equations are applicable to FRM filters synthesized with other nonlinear optimization techniques [26]–[28], [31], [33], [34], [38] although they are derived based on the FRM filters designed by the SQP technique. The reason is that the use of nonlinear optimization techniques is intended to produce a globally optimized design, e.g., a filter with a minimum number of coefficients satisfying the given specifications. Hence, no matter what methods are used, the resulting FRM filters should approach the same destination, i.e., the final filter could be quite similar. One of the evidences is example IV [31]. The filter is optimized by the second algorithm of Dutta and Vidyasagar, yet the actual design agrees well with the proposed equations.

7. Conclusions

In this paper, we have presented a set of new design equations for the estimation of the length of the bandedge shaping filter, the total length of two masking filters, and the optimum interpolation factor for a jointly optimized FRM filter. It is shown that an accurate optimum interpolation factor can be found if Kaiser's filter length estimation formula is modified for the bandedge shaping filter and the total length of the masking filters. Design examples confirmed the accuracy of the proposed design equations.

References

[1] L. C. R. de Barcellos, S. L. Netto, and P. S. R. Diniz, Optimization of FRM filters using the WLS-Chebyshev approach, *Circuits, Systems, and Signal Processing*, vol. 22, no. 2, pp. 99–113, Mar. 2003.

[2] R. Brayton, S. Director, G. Hachtel, and L. Vidigal, A new algorithm for statistical circuit design based on quasi-newton methods and function splitting, *IEEE Trans. Circuit Syst.*, vol. 26, no. 9, pp. 784–794, Sep. 1979.

[3] L. Cen and Y. Lian, Hybrid genetic algorithm for the design of modified frequency-response masking filters in a discrete space, *Circuits, Systems, and Signal Processing*, vol. 25, no. 2, pp. 153–174, Apr. 2006.

[4] C. K. Chen and J. H. Lee, Design of sharp-cutoff FIR digital filters with prescribed constant group delay, *IEEE Trans. Circuit Syst. II*, vol. 43, pp. 1–13, Jan. 1996.

[5] S. W. Foo and W. T. Lee, Application of fast filter bank for transcription of polyphonic signals, *Circuits, Systems, and Computers*, vol. 12, no. 5, pp. 655–674, Oct. 2003.

[6] M. B. Furtado Jr., P. S. R. Diniz, and S. L. Netto, Optimized prototype filter based on the FRM approach for cosine-modulated filter banks, *Circuits, Systems, and Signal Processing*, vol. 22, no. 2, pp. 193–210, Mar. 2003.

[7] O. Gustafsson, H. Johansson and L. Wanhammar, Single filter frequency masking high-speed recursive digital filters, *Circuits, Systems, and Signal Processing*, vol. 22, no. 2, pp. 219–238, Mar. 2003.

[8] O. Gustafsson, H. Johansson, and L. Wanhammar, Single filter frequency-response masking FIR filter, *Circuits, Systems, and Computers*, vol. 12, no. 5, pp. 601–630, Oct. 2003.

[9] H. Johansson, Two classes of frequency-response masking linear-phase FIR filters for interpolation and decimation, *Circuits, Systems, and Signal Processing*, vol. 25, no. 2, pp. 175–200, Apr. 2006.

[10] H. Johansson and T. Saramäki, Two-channel FIR filter banks utilizing the FRM approach, *Circuits, Systems, and Signal Processing*, vol. 22, no. 2, pp. 157–192, Mar. 2003.

[11] J. F. Kaiser, Nonrecursive digital filter design using I_0-sinh window function, *Proceedings of IEEE Int. Symp. on Circuits Syst.*, pp. 20–23, Apr. 1974.

[12] W. R. Lee, V. Rehbock, and K. L. Teo, Frequency-response masking based FIR filter design with power-of-two coefficients and suboptimum PWR, *Circuits, Systems, and Computers*, vol. 12, no. 5, pp. 591–600, Oct. 2003.

[13] W. R. Lee, V. Rehbock, and K. L. Teo, A weighted least-square-based approach to FIR filter design using the frequency-response masking technique, *IEEE Signal Processing Letters*, vol. 11, pp. 593–596, Jul. 2004.

[14] Y. Lian, The optimum design of half-band filter using multi-stage frequency-response masking technique, *Signal Processing*, vol. 44, no. 7, pp. 369–372, Jul. 1995.

[15] Y. Lian, Complexity reduction for FRM-based FIR filters using the prefilter-equalizer technique, *Circuits, Systems, and Signal Processing*, vol. 22, no. 2, pp. 137–155, Mar. 2003.

[16] Y. Lian, A modified frequency response masking structure for high-speed FPGA implementation of programmable sharp FIR filters, *Circuits, Systems, and Computers*, vol. 12, no. 5, pp. 643–654, Oct. 2003.

[17] Y. Lian and Y. C. Lim, Reducing the complexity of frequency-response masking filters using half band filters, *Signal Processing*, vol. 42, no. 3, pp. 227–230, Mar. 1995.

[18] Y. Lian and C. Z. Yang, Complexity reduction by decoupling the masking filters from the bandedge shaping filter in the FRM technique, *Circuits, Systems, and Signal Processing*, vol. 22, no. 2, pp. 115–135, Mar. 2003.

[19] Y. Lian, L. Zhang, and C. C. Ko, An improved frequency response masking approach for designing sharp FIR filters, *Signal Processing*, vol. 81, pp. 2573–2581, Dec. 2001.

[20] Y. C. Lim, Frequency-response masking approach for the synthesis of sharp linear phase digital filters, *IEEE Trans. Circuits Syst.*, vol. 33, pp. 357–364, Apr. 1986.

[21] Y. C. Lim and Y. Lian, The optimum design of one- and two-dimensional FIR filters using the frequency response masking technique, *IEEE Trans. Circuits Syst. II*, vol. 40, pp. 88–95, Feb. 1993.

[22] Y. C. Lim and Y. Lian, Frequency-response masking approach for digital design: complexity reduction via masking filter factorization, *IEEE Trans. Circuits Syst. II*, vol. 41, pp. 518–525, Aug. 1994.

[23] Y. C. Lim and R. Yang, On the synthesis of very sharp decimators and interpolators using the frequency-response masking technique, *IEEE Trans. Signal Processing*, vol. 53, no. 4, pp. 1387-1397, Apr. 2005.

[24] Y. C. Lim, Y. J. Yu, H. Q. Zheng, and S. W. Foo, FPGA implementation of digital filters synthesized using FRM technique, *Circuits, Systems, and Signal Processing*, vol. 22, no. 2, pp. 211–218, Mar. 2003.

[25] Y. Z. Liu and Z. P. Lin, On the applications of the frequency-response masking technique in array beamforming, *Circuits, Systems, and Signal Processing*, vol. 25, no. 2, pp. 201–224, Apr. 2006.

[26] W. S. Lu and T. Hinamoto, Optimal design of frequency-response-masking filters using semidefinite programming, *IEEE Trans. Circuits Syst. I*, vol. 50, pp. 557–568, Apr. 2003.

[27] W. S. Lu and T. Hinamoto, Optimal design of FIR frequency-response-masking filters using second-order cone programming, *The Proceedings of IEEE Int. Symp. on Circuits Syst.*, vol. 3, pp. 878-881, May, 2003.

[28] W. S. Lu and T. Hinamoto, Optimal design of IIR frequency-response-masking filters using second-order cone programming, *IEEE Trans. Circuits Syst. I*, vol 50, pp. 1401–1412, Nov. 2003.

[29] S. L. Netto, L. C. R. de Barcellos, and P. S. R. Diniz, Efficient design of narrowband cosine-modulated filter banks using a two-stage frequency-response masking approach, *Circuits, Systems, and Computers*, vol. 12, no. 5, pp. 631–642, Oct. 2003.

[30] Y. Neuvo, Dong Cheng-Yu, and S. K. Mitra, Interpolated finite impulse response filters, *IEEE Trans. Acoust., Speech, Signal Processing*, vol. 32, pp. 563–570, Jun. 1984.

[31] T. Saramäki and H. Johansson, Optimization of FIR filters using the frequency-response masking approach, *Proceeding of IEEE Int. Symp. on Circuits Syst.*, vol. 2, pp. 177–180, May 2001.

[32] T. Saramäki and Y. C. Lim, Use of the Remez algorithm for designing FRM based FIR filters, *Circuits, Systems, and Signal Processing*, vol. 22, no. 2, pp. 77–97, Mar. 2003.

[33] T. Saramäki and J. Yli-Kaakinen, Optimization of frequency-response-masking based FIR filters with reduced complexity, *The Proceedings of IEEE Int. Symp. on Circuits Syst.*, vol. 3, pp. 225–228, May 2002.

[34] T. Saramäki, J. Yli-Kaakinen, and H. Johansson, Optimization of frequency-response masking based FIR filters, *Circuits, Systems, and Computers*, vol. 12, no. 5, pp. 563–590, Oct. 2003.

[35] C. Z. Yang and Y. Lian, A modified structure for the design of sharp FIR filters using frequency response masking technique, *Proceeding of IEEE Int. Symp. on Circuits Syst.*, vol. 3, pp. 237–240, May 2002.

[36] R. H. Yang, B. Liu, and Y. C. Lim, A new structure of sharp transition FIR filters using frequency-response masking, *IEEE Trans. Circuits Syst.*, vol. 35, pp. 955–966, Aug. 1988.

[37] J. H. Yu and Y. Lian, Frequency-response masking based filters with the even-length bandedge shaping filter, *The Proceeding of IEEE Int. Symp. on Circuits Syst.*, vol. 5, pp. 536–539, May 2004.

[38] Y. J. Yu and Y. C. Lim, FRM based FIR filter design—the WLS approach, *The Proceeding of IEEE Int. Symp. on Circuits Syst.*, vol. 3, pp. 221–224, May 2002.